UDC 539.4

# Stacking Layer Sequence Effects for Glass Fibre/Epoxy Resin Cross-Ply Laminates

**E. H. Harkati,[a] A. Bezazi,[b,c] M. Guenfoud,[d] and F. Scarpa[b]**

[a] Département de Génie Civil, Université de Tébessa, Tébessa, Algérie

[b] Department of Aerospace Engineering, University of Bristol, Bristol, UK

[c] Laboratoire de Mécanique et Structure (LMS), Université de Guelma, Algérie

[d] Laboratoire de Génie Civil et d'Hydraulique (LGCH), Département de Génie Civil, Université de Guelma, Algérie

УДК 539.4

# Влияние последовательности укладки слоев на механические характеристики многослойных ламинатов из стекловолокна–эпоксидной смолы

**Э. Х. Харкати[а], А. Безази[б,в], М. Гуэнфуд[г], Ф. Скарпа[б]**

[а] Отделение гражданского строительства, Университет г. Тебесса, Алжир

[б] Отделение аэрокосмической промышленности, Университет г. Бристоль, Великобритания

[в] Лаборатория механики и структуры, Университет г. Гуэльма, Алжир

[г] Лаборатория гражданского строительства и гидравлики, Университет г. Гуэльма, Алжир

*Оценивается влияние последовательности укладки слоев ламината на распределение полей деформаций и напряжений по его толщине. Ламинатные образцы состоят из слоев эпоксидной смолы и стекловолокон, причем соотношение слоев с ориентацией волокон от 0 до 90° равно единице. Такое соотношение слоев использовалось при изготовлении ламинатов различной толщины. Описано напряженно-деформированное состояние многослойных ламинатов при линейном статическом нагружении с помощью конечноэлементных моделей стандартных программных пакетов ANSYS 6.1 и LUSAS 15.3. Численное моделирование выполнено для случая трехточечного изгиба ламината. Выполнен расчет материала в вязкоупругом состоянии, основанный на принципе подобия. Результаты расчета методом конечных элементов хорошо согласуются с полученными в рамках классической теории ламинатов. Для конкретных значений модулей вязкоупругости и распределения различных параметров определена оптимальная последовательность укладки слоев применительно к динамическим задачам для таких конструкций, как ламинатные рессоры для новых автомобильных подвесных систем.*

***Ключевые слова***: многослойные ламинаты, трехточечный изгиб, конечноэлементные модели, численное моделирование, последовательность укладки слоев ламината.

**Introduction**. Traditional isotropic and homogeneous materials offer a limited choice in terms of degrees of freedom to design high-performance structures. Composite materials offer the flexibility, lightweight characteristics and high-end performance required nowadays in all constructions sectors, like aerospace, ship building, railway structures and, more recently, automotive applications. Advanced composites show high stiffness characteristics along preferential directions, good fatigue resistance, no presence of corrosion when the material components are not metallic, complex shape forming and decreasing manufacturing costs. Worldwide composite materials production is increasing at a 6% rate each year [1–2]. More recent applications of composite laminates are related to the design of novel spring leaves for automotive suspensions, such for the case of Renault minivans and the new Chevrolet Corvette.

The widespread use of composite laminates in different engineering fields involves the use, at design stage, or simplified formulas to speed-up the time to market of the product. However, some aspects of their behaviour under complex loading patterns are still insufficiently understood. The effect of the stacking layer sequence over the damage tolerance and fatigue the cross-ply laminates was studied by Bezazi et al. [3–5]. A three-dimensional analysis by finite elements showed that the stacking sequence affects the loss rate of energy [6]. The influence of the stacking layer sequence for the case of laminates $(0_m/90_n)_s$ and $(90_n/0_n)_s$ was studied by Sun and Jen [7] and El Mahi et al. [8] using finite element analysis. The last authors evaluated the loss of rigidity and energy in cross laminates during fatigue tests for tensile loading. A macromechanical approach was also used by Tsau and Liu [9] to study the effect of the stacking sequence over the stress distribution on the laminates. Using two methods of optimisation, the authors examined the optimal stacking for the symmetrical and non-symmetrical laminates. Park et al. [10] maximized the resistance of the composite laminates by using genetic algorithms to find the optimal stacking for various conditions of loading and border. A theoretical study was also carried out to optimise the design of the plates symmetrically laminated with regard to the orientation of fibres and the thickness of the layers [1]. In this work the authors showed that the optimal fibre orientation is single and independent of the order of stacking. Results were also obtained for the optimal thickness values of each layer. Tsai and Hahn [11] for the first time proposed the stacking sequences used in this work. However, they did not carry further analysis on the effects that these laminates have over the stress and strain field distributions in composite laminates under out-of-plane loading. This work is aimed at filling this gap, with the analysis of the effect of the stacking layer sequence over the internal stress and strain distribution for these classes of symmetric laminates, which are also denoted by ease of manufacturing. Moreover, the uses of simplified engineering formulation for composite beams under three-point bending loading (typical, for example, of spring-leaf solutions) are benchmarked against analysis provided by two different commercial FE codes based on different element formulations. An evaluation of the influence of these particular stacking sequences over the complex flexural modulus (i.e., hysteretic damping) of the composite laminate following a simplified beam formulation is also carried out. The rationale of this analysis is based on the importance that the material damping can provide to optimise the design of composite-based springs for suspension applications.

**Materials and Simulations.**

***Materials***. Figure 1 shows the different types of cross-ply laminates considered, the ST 1 $(0_4/90_4)$, ST 2 $[(0_2/90_2)_s]_s$, ST 3 $[(0_2/90_2)_2]_s$, and ST 4 $[(0/90)_4]_s$. The laminates were manufactured using glass fibres and epoxy resin, having all as many plies oriented at 0° as those oriented at 90°. The laminate components are provided by SICOMIN plc; their principal characteristics being given in [4]. The laminates were subjected to tensile tests using an universal monotonic hydraulic Instron 8516 tensile machine with 100 kN of load capacity. Five tests were carried out for each laminate at a feed rate of 2 mm/min. The values measured for the in-plane mechanical orthotropic properties are: $E_L$ = (34 to 37) GPa, $E_T$ = (8.5 to 9.0) GPa, $\nu_{LT} = 0.25$ and $G_{LT}$ = (4.4 to 5.5) GPa, where: $E_L$, $E_T$, $\nu_{LT}$, and $G_{LT}$ are, respectively, the longitudinal and transverse Young's modulus, the in-plane Poisson's ratio, and in-plane shear modulus.

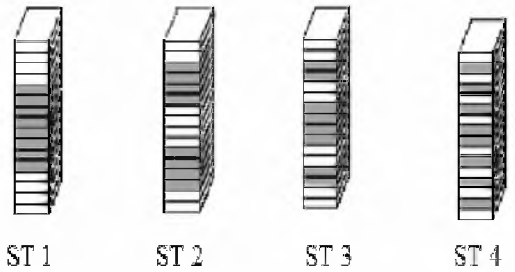


Fig. 1. Laminates considered in this work.

***Homogeneous Beam Model***. The mechanical behavior of the laminate beam can be identified using a simplified approach [12]. Considering a special orthotropic linear elastic material, Hooke's law can be expressed as

$$\begin{bmatrix} \sigma_{11} \\ \sigma_{22} \\ \sigma_{66} \end{bmatrix} = \begin{bmatrix} Q_{11} & Q_{12} & 0 \\ Q_{12} & Q_{22} & 0 \\ 0 & 0 & Q_{66} \end{bmatrix} \begin{bmatrix} \varepsilon_{11} \\ \varepsilon_{22} \\ \varepsilon_{66} \end{bmatrix}. \tag{1}$$

The in-plane stiffness constant $Q_{ij}$ can be formulated in terms of in-plane Young's moduli and Poisson's ratio:

$$\begin{aligned} Q_{11} &= \frac{E_L}{1 - \dfrac{E_T}{E_L}\nu_{LT}^2}, & Q_{22} &= \frac{E_T}{E_L} Q_{11}, \\ Q_{12} &= \nu_{LT} Q_{11}, & Q_{66} &= G_{LT}. \end{aligned} \tag{2}$$

Using a structural reference frame [12], Eq. (1) becomes:

$$\begin{bmatrix} \sigma_{xx} \\ \sigma_{yy} \\ \sigma_{xy} \end{bmatrix} = \begin{bmatrix} Q'_{11} & Q'_{12} & 0 \\ Q'_{12} & Q'_{22} & 0 \\ 0 & 0 & Q'_{66} \end{bmatrix} \begin{bmatrix} \varepsilon_{xx} \\ \varepsilon_{yy} \\ \gamma_{xy} \end{bmatrix}. \tag{3}$$

Introducing the classical matrix notation $A$, $B$, and $D$, one can identify the relation between in-plane forces and bending moments versus the tensile strain and curvature of the medium (neutral) plane of the laminate:

$$\begin{Bmatrix} N \\ M \end{Bmatrix} = \begin{bmatrix} A & B \\ B & D \end{bmatrix} \begin{Bmatrix} \varepsilon_m \\ \kappa_f \end{Bmatrix}, \tag{4}$$

where

$$A_{ij} = \sum_{k=1}^{n} (h_k - h_{k-1})(Q'_{ij})_k, \tag{5}$$

$$B_{ij} = \frac{1}{2} \sum_{k=1}^{n} (h_k^2 - h_{k-1}^2)(Q'_{ij})_k, \tag{6}$$

$$D_{ij} = \frac{1}{3} \sum_{k=1}^{n} (h_k^3 - h_{k-1}^3)(Q'_{ij})_k. \tag{7}$$

When the coupling matrix $B$ is non-zero, an in-plane load on the laminate plate can lead to a transversal displacement having the same magnitude of the in-plane one. The expressions of the in-plane stresses can be therefore rewritten using the external bending moment $M$ and inertia moment $I$ (rectangular section) as

$$\sigma_{xx}^k = z a_{xx}^k \frac{M}{I}, \tag{8a}$$

$$\sigma_{yy}^k = z a_{yy}^k \frac{M}{I}, \tag{8b}$$

$$\sigma_{xy}^k = z a_{xy}^k \frac{M}{I}, \tag{8c}$$

where

$$\begin{aligned} a_{xx}^k &= (Q_{11}^k D_{11}^* + Q_{12}^k D_{12}^* + Q_{16}^k D_{16}^*) \frac{h^3}{12}, \\ a_{yy}^k &= (Q_{12}^k D_{11}^* + Q_{22}^k D_{12}^* + Q_{26}^k D_{16}^*) \frac{h^3}{12}, \\ a_{xy}^k &= (Q_{16}^k D_{11}^* + Q_{26}^k D_{12}^* + Q_{66}^k D_{16}^*) \frac{h^3}{12}. \end{aligned} \tag{9}$$

Equations (9) are valid only away from the edges of the laminate for beam having aspect ratios $b/h$ higher than 16 [12]. In that case, the shear stress through the thickness at position $z$ under a shear loading $Q$ can be expressed as

$$\sigma_{xz} = \frac{3Q}{2bh}\left[1 - 4\left(\frac{z}{h}\right)^2\right]. \tag{10}$$

With the maximum shear stress at $z = 0$:

$$\sigma_{xz}(z=0) = \tau_0 = \frac{3Q}{2bh}. \tag{11}$$

Equation (10) is therefore rearranged as

$$\sigma_{xz} = -a_{xx}^k \tau_0 \left[4\left(\frac{z}{h}\right)^2 + d_k\right], \tag{12}$$

where $d_k$ are numerical constants to be determined assuming the continuity of $\sigma_{xz}$ through the beam thickness.

For a beam of length $L$ subjected to three-point bending the stresses for the $k$th layer can be written as

$$\begin{aligned} \sigma_{xx}^k &= -6a_{xx}^k \frac{P}{bh^3} xz, \\ \sigma_{yy}^k &= -6a_{yy}^k \frac{P}{bh^3} xz, \\ \sigma_{xy}^k &= -6a_{xy}^k \frac{P}{bh^3} xz. \end{aligned} \tag{13}$$

The maximum stresses occur at half-length of the beam, i.e.,

$$\begin{aligned} \sigma_{xx}^k &= -3a_{xx}^k \frac{P}{bh^3} z, \\ \sigma_{yy}^k &= -3a_{yy}^k \frac{P}{bh^3} z, \\ \sigma_{xy}^k &= -3a_{xy}^k \frac{P}{bh^3} z. \end{aligned} \tag{14}$$

For the case of an homogeneous isotropic material ($a_{xx} = 1$), the normal stress can be rewritten as

$$\sigma_{xx}^k = -\frac{3PL}{bh^3} z. \tag{15}$$

With the maximum normal stress being

$$\sigma_{xx\max}^k = \sigma_0 = \frac{3PL}{2bh^2}. \tag{16}$$

Following (15) and (16), the normal stress for each lamina can therefore be expressed as

$$\sigma_{xx}^{k} = -2a_{xx}^{k}\sigma_0 \frac{z}{h}. \tag{17}$$

The constants $c_k$ in each layer are determined zeroing the stress $\sigma_{xz}$ on the lower and upper skins and assuring continuity of $\sigma_{xz}$ across the laminate, obtaining therefore for the case of a homogeneous material:

$$\sigma_{xz} = \frac{Qh^2}{8I}\left[1 - 4\left(\frac{z}{h}\right)^2\right] = \frac{3Q}{2bh}\left[1 - 4\left(\frac{z}{h}\right)^2\right]. \tag{18}$$

The maximum shear stress is given by

$$\sigma_{xz}(z=0) = \tau_0 = \frac{3Q}{2bh}. \tag{19}$$

Inserting Eq. (19) in (12) one obtains, for a homogeneous material

$$\sigma_{xz} = \tau_0\left[1 - 4\left(\frac{z}{h}\right)^2\right]. \tag{20}$$

For a beam with equivalent homogenous and isotropic material the stress $\sigma_{xx}$ for each layer can be expressed as

$$\sigma_{xx}^{k} = -\frac{3PL}{bh^3} z. \tag{21}$$

With the maximum stress being equal to

$$\sigma_{xx\max}^{k} = \sigma_0 = \frac{3PL}{bh^2}. \tag{22}$$

***Flexural Complex Modulus***. The elastic-viscoelastic correspondence principle was first applied by Hashin [13] in the case of fibre-reinforced composites. The complex modulus approach considers a harmonic time variation of the applied stress and strains in the following form:

$$\varepsilon(t) = \varepsilon_0 e^{i\omega t}, \tag{23}$$

$$\sigma(t) = [C(\omega)]^{*}\varepsilon_0 e^{i\omega t}, \tag{24}$$

where $[C(\omega)]^{*}$ is the complex stiffness matrix obtained using the viscoelastic reciprocity principle. The effective complex flexural modulus for a laminate beam can therefore be expressed with the following formulation [14]:

$$E_f^* = \frac{12}{h^3 D_{11}^{*-1}}, \tag{25}$$

where the flexural complex modulus can be divided into real and imaginary part:

$$E_f^* = \overline{E}_f(1 + i\eta_f), \tag{26}$$

where $\eta_f$ is the loss factor for the flexural modulus. Considering curvature-moment corrections [15], the effective complex flexural modulus can be expressed as

$$E_{fe}^* = \frac{1}{1 - \dfrac{(D_{16}^{*-1})^2}{D_{11}^{*-1} D_{66}^{*-1}}} E_f^*. \tag{27}$$

***Finite-Element Simulations – Static Three-Point Bending Loading***. The finite-element (FE) simulations of the three-point bending loading have been performed using the SHELL93 elements of the commercial code ANSYS 6.1, and the QTS8 element from the code LUSAS 13.5. The latter code uses a Total Lagrangian formulation for medium and thick shells, which is based on the degeneration of a 3D continuum. In this approach, the displacements at any point in the shell are defined by the translation of the reference surface together with the rotation of a director. The director is subsequently referred to as the normal, however, the director need not be initially normal to the reference surface. The normal is considered to remain straight during deformation for computation of displacements through the element thickness. The quadrilateral element QTS8 adopts an assumed strain field for interpolation of the transverse shear strains. The inclusion of an assumed strain field prevents the element from 'shear locking' when used as a thin shell. The SHELL93 ANSYS element has normal to the centre-plane assumed to remain straight after deformation, but not necessarily normal to the centre-plane itself. Also, SHELL93 element has no significant stiffness associated with rotation about the element normal axis. A nominal value of stiffness is present, however, to prevent free rotation at the node. For the three-point bending case, the specific geometry on the beams and the stacking sequences layouts allow to model only 1/8th of the beam itself (Fig. 2). Therefore, only 8 laminas are modelled, each consisting of 3 orthotropic layers having single thickness of 0.0833 mm. Both for the ANSYS and LUSAS models, the mesh consisted in 525 elements with 6 DOFs per node. The calculations were performed on an Windows-based PC with 2 GHz of processor and 1 GB of RAM.

**Results and Discussions**. Figure 3 shows the comparison between the stress ratio $\sigma_{xx}/\sigma_0$ for the different stacking sequences considered, calculated dividing Eqs. (21) and (22), and using the FE simulations as well as results from the classical laminate theory (CLT). It is evident from the figures that the use of approximate design formulas (21) and (22) leads to averaging the stresses over the thickness with a linear variation, therefore introducing considerable errors

compared to the FE simulations and the CLT predictions. The maximum values for $\sigma_{xx}/\sigma_0$ are for the laminate ST4 $[(0/90)_4]_s$ (Fig. 3d), the one presenting the lower number of layers with the same orientation. The other laminates are classified following the number of layers possessing the same orientation: ST 3 $[(0_2/90_2)_2]_s$, ST 2 $[(0_2/90_2)_s]_s$, and ST 1 $[(0_4/90_4)]$.

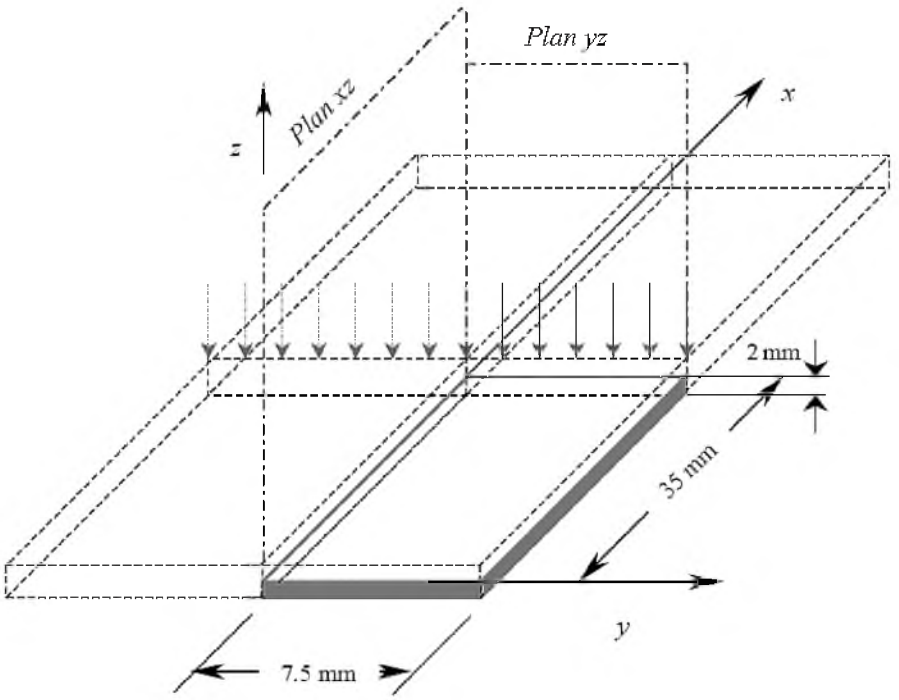


Fig. 2. Laminate beam under three-point bending loading.

Figure 4 shows the variation of stresses $\sigma_{yy}/\sigma_0$ over the thickness of the laminates. The stresses are maximum a the interface with the layers oriented at zero degrees, with positive values for lamina at 0° and negative at 90° of orientation. It is noteworthy that the values are decreased by a factor of 20 compared to the stresses $\sigma_{xx}/\sigma_0$ illustrated before.

Figure 5 shows the ratio $\sigma_{xz}/\sigma_0$ of through the laminates thickness. The maximum values lie on the axis of symmetry of the laminate, corresponding to the neutral plane of the composite. The ANSYS FE model follows closely the homogeneous beam model, offering higher discrepancies with the CLT predictions for the laminates ST4 and ST3. The laminates with the lowest number of plies having the same orientation offer the lowest values of the shear stresses.

Figure 6 shows the strain fields $\varepsilon_{xx}$ and $\varepsilon_{yy}$ for the four laminates. The values of $\varepsilon_{xx}$ are positive, while the $\varepsilon_{yy}$ ones are negative. Both strain fields provide a linear variation through the thickness of the laminates from 0 at the axis of symmetry to maximum values at the ends of the composite beams. The strain fields are more important in terms of magnitude for the laminates with the highest number of equal orientation plies. The average ratio between $\varepsilon_{xx}$ and $\varepsilon_{yy}$ strains is 10.

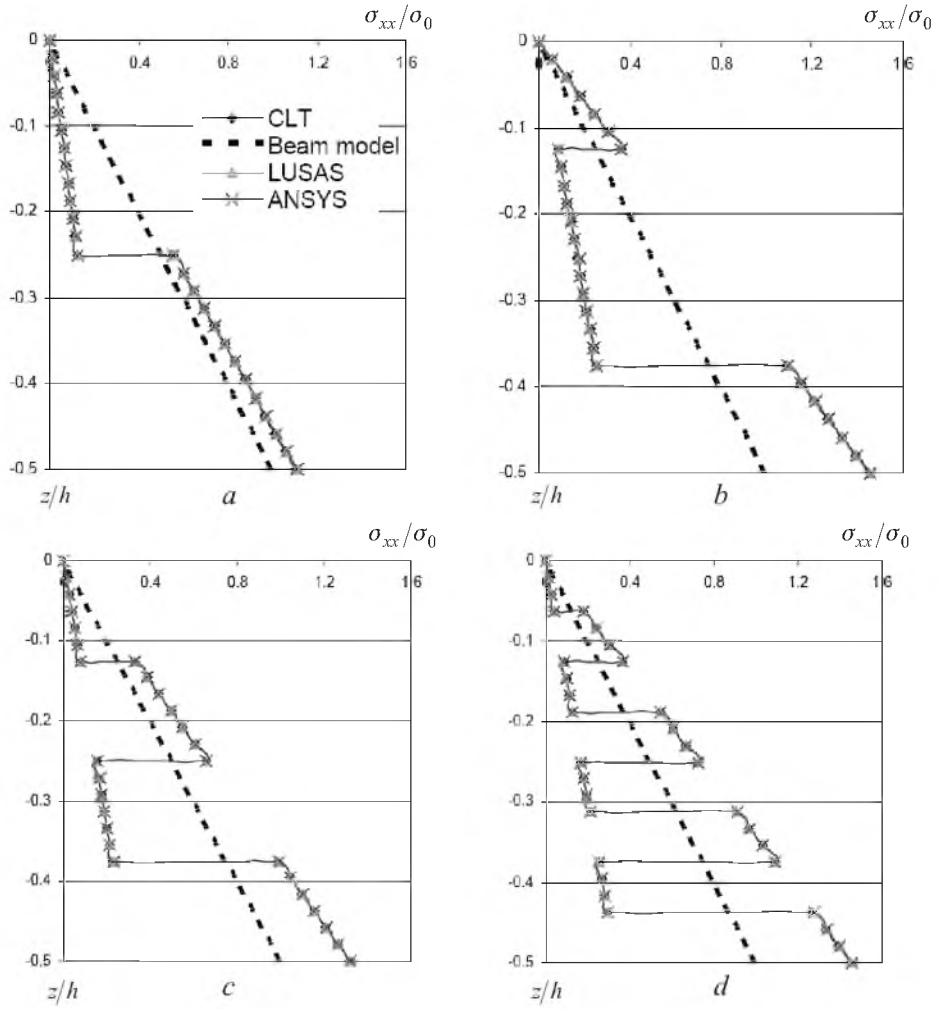


Fig. 3. Through-the-thickness stress ratio $\sigma_{xx}/\sigma_0$ distribution for the different laminates.

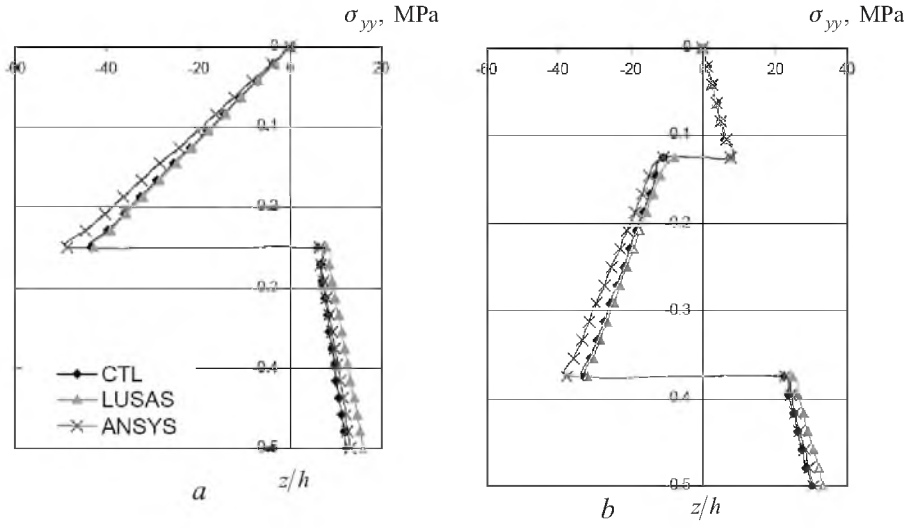

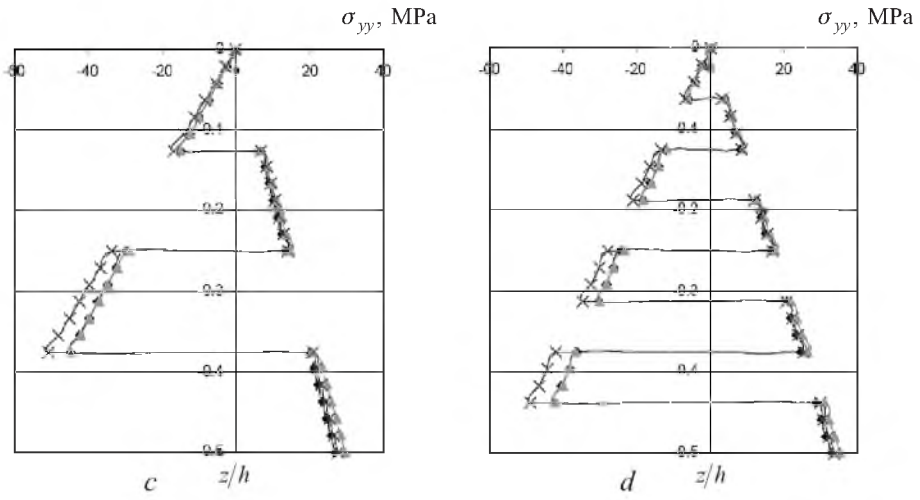


Fig. 4. Through-the-thickness stress $\sigma_{yy}$ distribution for the different laminates.

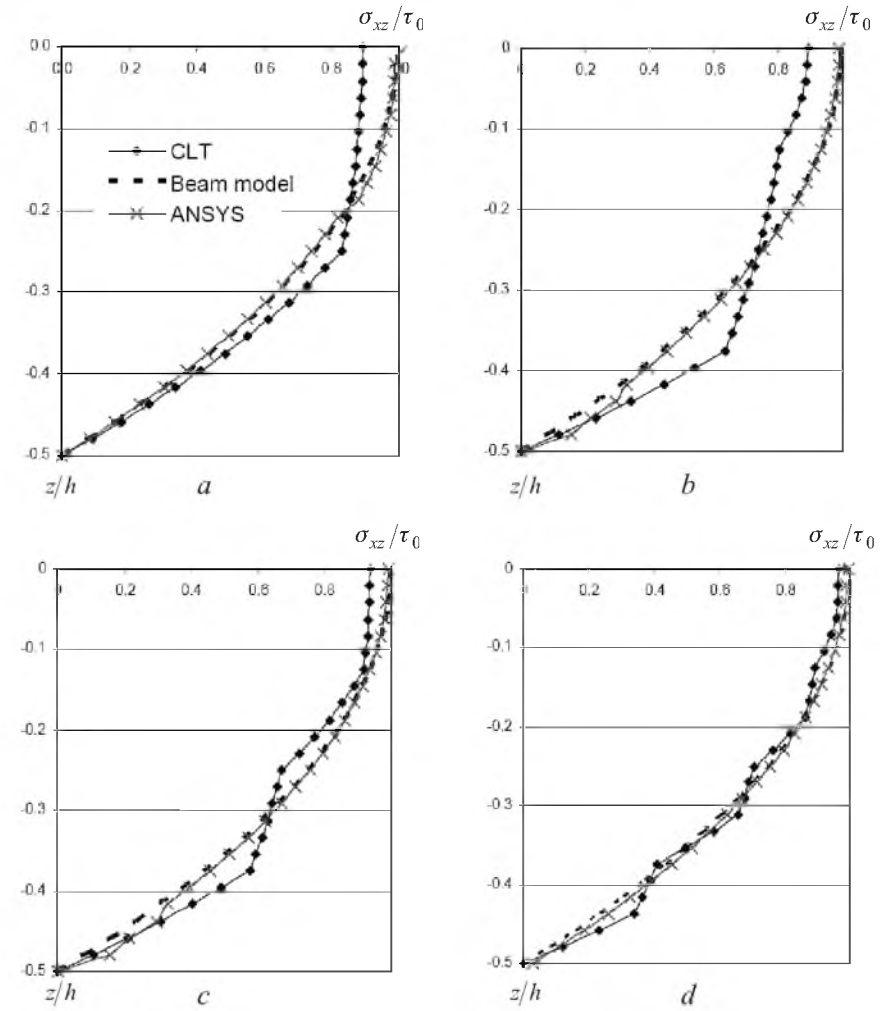


Fig. 5. Through-the-thickness stress ratio $\sigma_{xz}/\tau_0$ distribution for the different laminates.

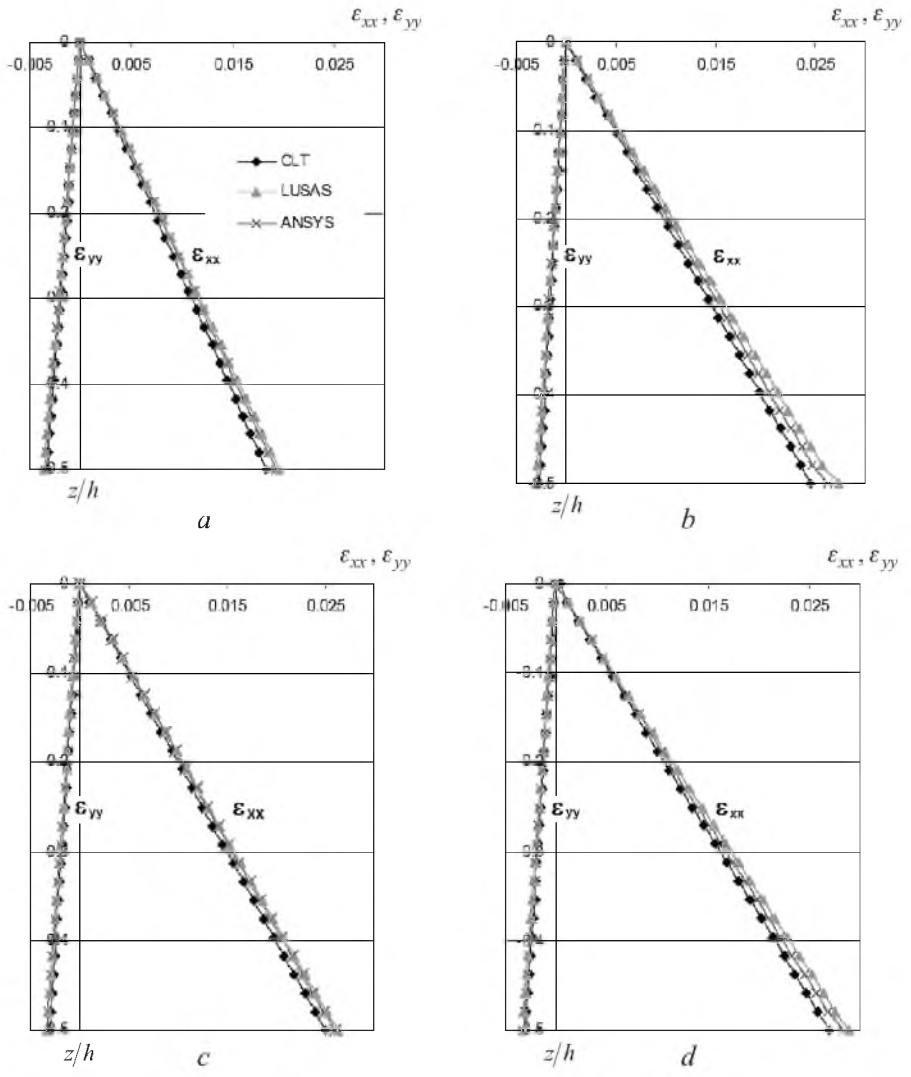


Fig. 6. Evolution of strain fields through the thickness of the laminates.

Table 1 shows a comparison between the storage modulus and loss factors for the four laminates considered. The loss factors are all confined between 1.66 and 1.70%, with no significant dependence of the loss modulus versus the stacking sequence topology. On the other hand, the storage modulus of laminate ST1 is significantly higher (50.4 GPa) compared to the one of ST3 (46.6 GPa) and ST2 and ST3 (44.6 GPa). In view of possible applications as spring leaf devices, if lower natural frequencies are sought, the ST3 laminate seems to offer the best compromise in terms both of viscoelastic properties and through-the-thickness stress and strain distributions. Moreover, the ST3 laminate has been experimentally proven as the best suited for three-point bending fatigue loading [4]. The laminate ST1 and ST3 provide also the lowest maximum normal stresses and strains through-the-thickness, an interesting feature for structural integrity-oriented applications.

Table 1

**Storage Modulus and Loss Factors for the Various Laminates**

| Laminate | Flexural storage modulus (GPa) | Loss factor (%) |
|---|---|---|
| ST1 | 50.4 | 1.66 |
| ST2 | 44.6 | 1.70 |
| ST3 | 46.6 | 1.68 |
| ST4 | 44.6 | 1.70 |

**Conclusions**. A finite element method is used to analyze the influence of the stacking sequence on the distributions of the stress and strain fields of specific cross-ply laminates in linear three-point bending. The analysis of the results obtained shows that the distribution of the stress depends on the type of stacking sequence, and that the homogeneous beams formulations used at initial design stage need to be backed by more refined analysis to determine accurate stress and strain fields. Stress $\sigma_{xx}$ and strain $\varepsilon_{xx}$ are most significant; the former being almost 20 times larger than the $\sigma_{yy}$ ones, while the latter are 10 times more significant than the strains $\varepsilon_{yy}$. The maximum stresses ($\sigma_{xx}$ and $\sigma_{yy}$) are located at the extremities of the laminates, and this is the same for the maximum deformations ($\varepsilon_{xx}$ and $\varepsilon_{yy}$). On the other hand, the maximum shear stress $\sigma_{xz}$ are localized in the middle of the beam. Using the reciprocity principle in viscoelasticity and the complex modulus approach, the various laminates provide comparable loss factor values lower than 2% and, apart one specific case of laminate, comparable storage flexural modulus.

**Резюме**

Оцінюється вплив послідовності укладання шарів ламіната на розподіл полів деформацій і напружень по його товщині. Ламінатні зразки складаються із шарів епоксидної смоли і скловолокна, при цьому співвідношення шарів з орієнтацією волокон від 0 до 90° дорівнює одиниці. Таке співвідношення шарів використовувалося при виготовленні ламінатів різної товщини. Описано напружено-деформований стан багатошарових ламінатів при лінійному статичному навантаженні за допомогою скінченноелементних моделей стандартних програмних пакетів ANSYS 6.1 та LUSAS 15.3. Числове моделювання виконано для триточкового згину ламіната. Проведено розрахунок матеріалу у в'язко-пружному стані, що базується на принципі подібності. Результати розрахунків методом скінченних елементів добре узгоджуються з отриманими у рамках класичної теорії ламінатів. Для конкретних значень модулей в'язко-пружності і розподілу різних параметрів визначено послідовність укладання шарів стосовно динамічних задач для таких конструкцій, як ламінатні ресори для нових автомобільних підвісних систем.

1. M. Avalle and G. Belingardi, "A theoretical approach to the optimization of flexural stiffness of symmetric laminates," *Compos. Struct.*, **31**, 75–86 (1995).

2. H. Chalaye, "Les matériaux composites. Dynamisme et innovation. SESSI, service de la direction générale de l'industrie, des technologies de l'information et des postes (DiGITIP)," Les 4 pages des statistiques industrielles, No. 158 (février 2002).
3. A. Bezazi, A. El Mahi., J.-M. Berthelot, et B. Bezzazi, "Analyse de l'endommagement des stratifiés en flexion 3-points. Influence de la séquence d'empilement," XVème Congrès Français de Mécanique (Nancy, 3–7 septembre) (2001).
4. A. Bezazi, A. El Mahi, J.-M. Berthelot, and B. Bezzazi, "Flexural fatigue behavior of cross-ply laminates: An experimental approach," *Strength Mater.*, **35**, No. 2, 149–161 (2003).
5. A. Bezazi, A. El Mahi, J.-M. Berthelot, and A. Kondratas, "Investigation of cross-ply laminates behavior in three-point bending tests. Part II: Cyclic fatigue tests," *Mat. Sci.*, **9**, No. 1, 128–133 (2003).
6. B. D. Davidson, R. Kruige, and M. Konig, "Three-dimensional analysis of center-delaminated unidirectional and multidirectional single-leg bending specimens, *Compos. Sci. Technol.*, **54**, 385–394 (1995).
7. C. T. Sun and K. C. Jen, "On the effect of matrix cracks on laminate strength," *J. Reinf. Plast. Comp.*, **6**, 208–223 (1987).
8. A. El Mahi, J.-M. Berthelot, and J. Brillaud, "Stiffness reduction and energy release rate of cross-ply laminates during fatigue tests," *Compos. Struct.*, **30**, Issue 2, 123–130 (1995).
9. L.-R. Tsau and C.-H. Liu, "A comparison between two optimisation methods on the stacking sequence of fibres-reinforced composite laminate," *Compos. Struct.*, **55**, Issue 3, 515–525 (1995).
10. J.-H. Park, J.-H. Hwang, C.-S. Lee, and W. Hwang, "Stacking sequence of composite laminates for maximum strength using genetic algorithms," *Compos. Struct.*, **52**, Issue 2, 217–231 (2001).
11. S. W. Tsai and H. T. Hahn, *Introduction to Composite Materials*, Technomic Publishing Co., Inc. Lancaster Basel (1980).
12. J.-M. Berthelot, *Composite Materials. Mechanical Behavior and Structural Analysis*, Springer, New York (1999).
13. Z. Hashin, "Complex modulus of viscoelastic composites. II. Fiber reinforced material," *Int. J. Solids Struct.*, **6**, 797–807 (1970).
14. R. B. Adams and D. C. G. Bacon, "Effect of fiber orientation and laminate geometry on the dynamic properties of CFRP," *J. Compos. Mater.*, **7**, 402–408 (1973).
15. J.-M. Berthelot and Y. Sefrani, "Damping analysis of unidirectional glass and Kevlar composites," *Compos. Sci. Technol.*, **64**, 1–18 (2004).

Received 16. 01. 2006